ACS chemical biology

Articles

Cite This: ACS Chem. Biol. 2019, 14, 526–533

pubs.acs.org/acschemicalbiology

Toolbox of Diverse Linkers for Navigating the Cellular Efficacy Landscape of Stapled Peptides

Yuteng Wu,[†] Amandeep Kaur,[§] Elaine Fowler,[†] Mareike M. Wiedmann,[†] Reginald Young,[‡] Warren R. J. D. Galloway,[†] Lasse Olsen,[†] Hannah F. Sore,[†] Anasuya Chattopadhyay,[∥] Terence T.-L. Kwan,[†] Wenshu Xu,[∥] Stephen J. Walsh,[†] Peterson de Andrade,[†] Matej Janecek,[†] Senthil Arumugam,[§] Laura S. Itzhaki,[∥] Yu Heng Lau,*[,‡] and David R. Spring*[,†]

[†]Department of Chemistry, University of Cambridge, Lensfield Road, Cambridge CB2 1EW, United Kingdom

[‡]School of Chemistry, The University of Sydney, Eastern Avenue, Sydney, NSW 2006, Australia

[§]European Molecular Biology Laboratory Australia Node for Single Molecule Science and ARC Centre of Excellence in Advanced Molecular Imaging, School of Medical Sciences, University of New South Wales, Sydney, NSW 2052, Australia

[∥]Department of Pharmacology, University of Cambridge, Tennis Court Road, Cambridge CB2 1PD, United Kingdom

Supporting Information

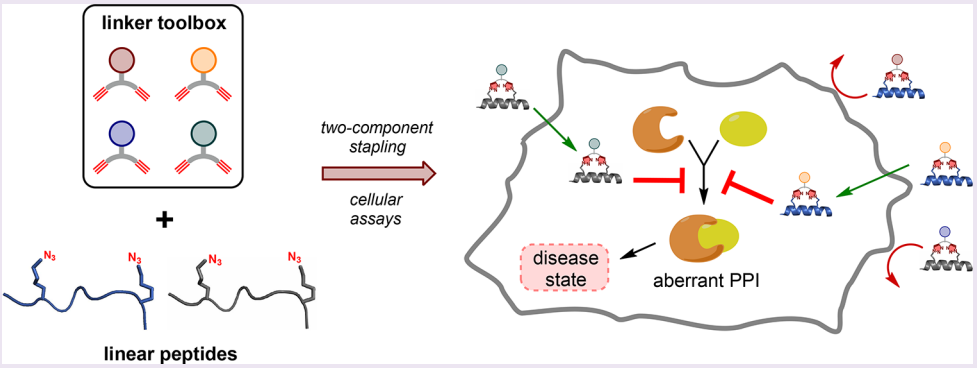

ABSTRACT: Stapled peptides have great potential as modulators of protein−protein interactions (PPIs). However, there is a vast landscape of chemical features that can be varied for any given peptide, and identifying a set of features that maximizes cellular uptake and subsequent target engagement remains a key challenge. Herein, we present a systematic analysis of staple functionality on the peptide bioactivity landscape in cellular assays. Through application of a "toolbox" of diversified dialkynyl linkers to the stapling of MDM2-binding peptides via a double-click approach, we conducted a study of cellular uptake and p53 activation as a function of the linker. Minor changes in the linker motif and the specific pairing of linker with peptide sequence can lead to substantial differences in bioactivity, a finding which may have important design implications for peptide-based inhibitors of other PPIs. Given the complexity of the structure−activity relationships involved, the toolbox approach represents a generalizable strategy for optimization when progressing from *in vitro* binding assays to cellular efficacy studies.

INTRODUCTION

Protein−protein interactions represent an exceptionally rich source of new potential drug targets. They are involved in all essential cellular processes, and aberrant PPIs are associated with many human diseases, such as cancer.[1−3] However, traditional small molecule library approaches are often not ideal for modulating PPI interfaces.[3−6]

A promising strategy that has generated significant interest within the scientific community is peptide stapling, in which a linear peptide is cross-linked via the formation of a linking motif (the "staple") between two of its side chains.[7,8] Stapling can constrain peptides into their bioactive conformation, and when optimized, can generate potent *in vivo* inhibitors of intracellular PPI targets.[9−12] However, cellular uptake mechanisms are currently not well understood, and cell permeability represents the major challenge when pursuing this type of modality as therapeutics.[6,13] Peptide sequence, charge, and staple type have all been implicated as important variables for cell penetration,[7,14−17] and design strategies such as guanidium and amphipathic patterning have emerged as promising ways to promote endocytic uptake and release.[18] Despite these advances, studies on inhibitor optimization for intracellular PPI targets are typically laborious and largely empirically driven, relying on extensive peptide synthesis and evaluation.

An emerging paradigm is the importance of the linker component of stapled peptides. In addition to performing

Received: January 21, 2019
Accepted: January 31, 2019
Published: January 31, 2019

DOI: 10.1021/acschembio.9b00063
ACS Chem. Biol. 2019, 14, 526−533

dynamic functions,[19−21] judicious selection of the linker from a library of potential options is a key consideration for achieving optimal bioactivity.[22−24] Although the archetypal stapling technique utilizes ring-closing metathesis on olefinic amino acids to form "all-hydrocarbon" stapled peptides,[11,25,26] a range of alternative stapling chemistries is now available.[8] Notably, two-component reactions allow the staple and peptide to be varied independently of each other, enabling facile access to greater diversity of stapled peptides (Figure 1).[22,27−31] We

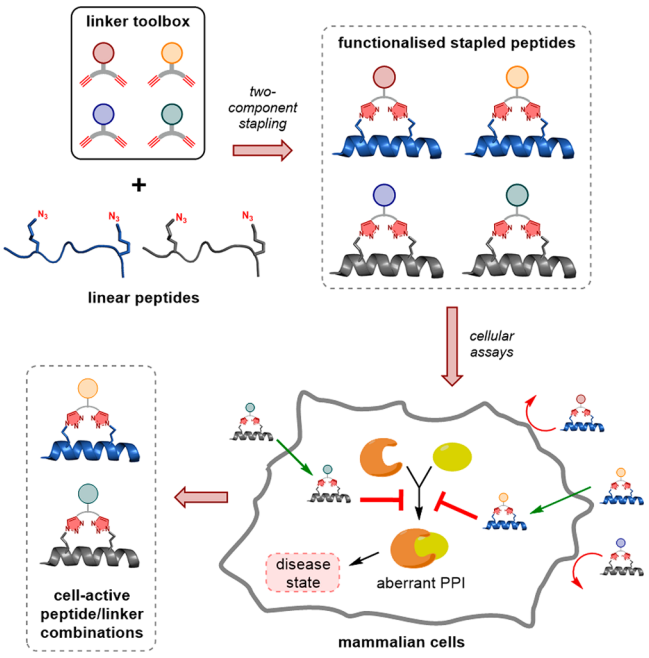

Figure 1. A linker toolbox for identifying bioactive peptide-linker combinations. Two-component stapling chemistry enables a range of functionalized dialkynyl linkers to be efficiently introduced, generating peptides with a range of chemical and biological properties. Subtle differences in the sequence and linker can lead to major differences in terms of activity in cellular assays.

previously established a double-click protocol for two-component stapling between diazidopeptides and dialkynyl linkers.[27,32] Drawing inspiration from cell-penetrating cationic peptides, we showed that cellular activity could be induced by using linker **1** that was functionalized with a triarginine motif (Figure 2). This strategy was used to design a cell-active inhibitor of the p53/MDM2 interaction, a validated drug target for the treatment of cancers that have wild-type p53 and overexpressed MDM2.[33,34]

In this work, we expand upon the limited set of functionalized dialkynyl linkers evaluated in previous studies.[23,27,35] A collection of 18 linkers **2**−**19** covering a wide range of functional motifs were applied to generate a small diverse library of new MDM2 inhibitors (Figure 2), providing valuable insights into the physicochemical factors that determine the cellular uptake and efficacy of stapled peptides. This linker collection has been used to study uptake in human platelets,[36] and its application to MDM2 inhibition serves to extend the generality of this "toolbox" for developing cell permeable stapled peptide inhibitors of other intracellular PPIs, tuning the efficacy through selection of the appropriate combination of staple linker and peptide sequence.

RESULTS AND DISCUSSION

Amino Acid Functionalized Linkers. With the previously reported triarginine R3 linker **1** as the starting point of our investigation, we began by exploring linkers bearing different types of amino acids, covering acidic (Glu), basic (Lys, His), polar (Ser), and hydrophobic (Leu) residues. Staples **2**−**6** were synthesized by solid-phase peptide synthesis and N-terminal capping with 3,5-diethynylbenzoic acid (Figure 2). The linkers were subsequently combined with the p53-derived sequence **A**, a peptide which was unable to activate cellular p53 in its linear form or when stapled with an unfunctionalized 3,5-diethynylbenzene linker.[27]

Stapled peptides **A2**−**A6** (i.e., peptide sequence **A** stapled with linkers **2**−**6**) were first evaluated for their ability to bind MDM2 *in vitro* using an established competitive fluorescence polarization assay (FP, Table 1).[27,37] All five peptides were found to have comparable low-nanomolar binding affinity for MDM2, indicating that the amino acid motifs did not interfere with target binding in an *in vitro* setting. The ability of stapled peptides **A2**−**A6** to activate cellular p53 was then assessed using a T22 mammalian reporter cell line previously used extensively by Lane and coworkers.[37] Hydrocarbon stapled peptides previously developed by Lane and coworkers were able to induce p53 activation at around 5−10 μM,[37] whereas the peptides in this study showed activation at 25 μM (the lowest concentration tested in the study). In contrast to the *in vitro* binding results, stapled peptide **A2** with the trilysine functionalized K3 linker **2** was the only active compound in the cellular reporter assay (Figure 3). This initial observation was consistent with previous reports indicating the importance of positive charge for cellular activity, although there are notable examples that do not conform to this trend.[35,38]

To further investigate the effect of net charge, linkers R3-OH **7** and K3-OH **8** were synthesized by solid-phase peptide synthesis on Wang resin to give the terminal acid functionalized linker analogues of **1** and **2**. Changing the amide to a negatively charged acid group resulted in loss of activity for both stapled peptides **A7** and **A8** in the p53 reporter assay (Figure 3), despite not affecting binding to MDM2 in the FP assay in the case of **A8** (Table 1). Extended tetrapeptide linkers R4 **9** and K4 **10** with an additional positive charge were also synthesized. While stapled peptide **A10** maintained a high affinity for binding MDM2 (Table 1), **A9** showed a decrease in apparent affinity in comparison to **A1**, potentially attributable to a less optimal peptide conformation (Supporting Information Figure S8.2.1). In the cellular reporter assay, K4 peptide **A10** showed an improved p53 response in comparison to K3 peptide **A2**, while **A9** showed no activity. In addition to a reduction in alpha helicity, the lack of activity with **A9** could also be due to poor solubility, as precipitation was observed in cell culture media during the assay (Figure 3 and Supporting Information Table S9.2.1). Together, these observations are consistent in suggesting that positive charge is an important requirement for the cellular activity of stapled peptides based on the wild-type p53 sequence.

We also explored the effect of amino acid modification by synthesizing side chain di- and trimethylated analogues **11** and **12** of the K3 linker **2**, as further cationic linker variants. Both modifications were again tolerated in terms of *in vitro* MDM2-binding but eliminated activity in cells. This result demonstrates that cationic charge alone is insufficient for cellular activity and reveals that primary amine functional groups have

DOI: 10.1021/acschembio.9b00063
ACS Chem. Biol. 2019, 14, 526−533

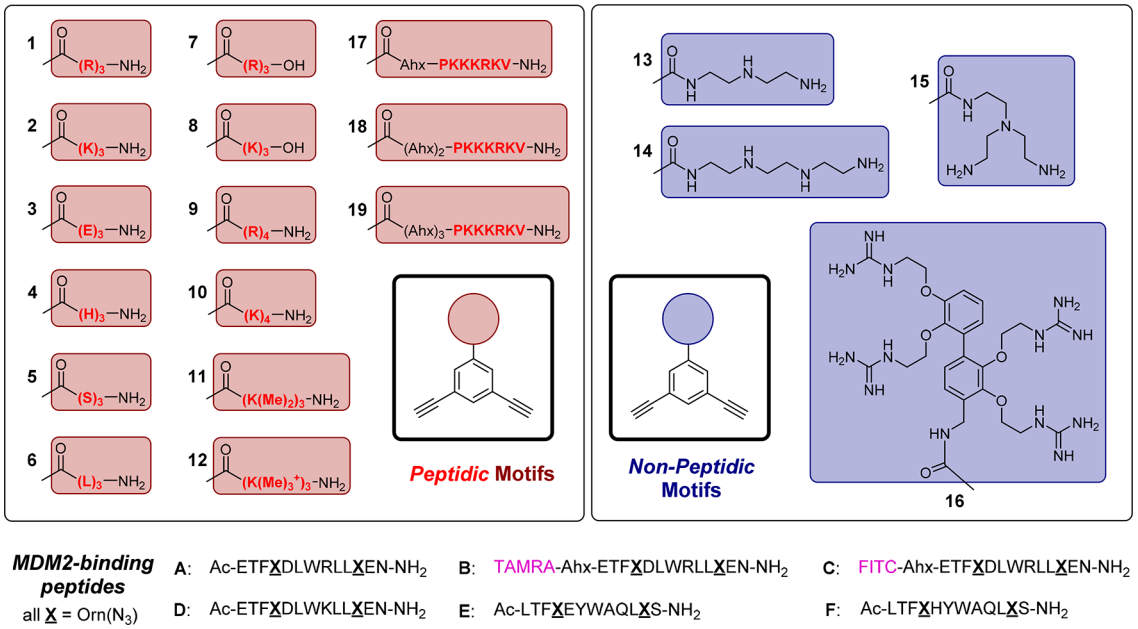

Figure 2. A toolbox of functionalized dialkynyl linkers **1**−**19** for generating stapled peptides with different cellular bioactivity. Linkers **1**−**12** feature amino acid motifs, **13**−**16** feature nonpeptidic cationic motifs, and **17**−**19** feature nuclear localization signal tags. In combination with MDM2-binding peptides **A**−**F**, a small diverse library of stapled peptides was synthesized and evaluated in cell-based assays for p53 activation.

Table 1. *In Vitro* Binding Affinities of Stapled Peptides A1−A19 (Peptide Sequence A Stapled with Linkers 1−19) for MDM2 as Measured by Fluorescence Polarization[b]

peptides	MDM2 K_i (nM)	peptides	MDM2 K_i (nM)
wt $p53_{17-29}$	821 ± 56[a]	A10	12 ± 1
A	16 ± 1[a]	A11	9.1 ± 0.8
A1	12 ± 1	A12	6.7 ± 0.6
A2	10 ± 1	A13	5.9 ± 0.7
A3	3.0 ± 0.4	A14	7.0 ± 0.8
A4	5.2 ± 0.6	A15	5.7 ± 0.7
A5	3.7 ± 0.4	A16	61 ± 9
A6	6.2 ± 0.6	A17	40 ± 6
A7	39 ± 2	A18	48 ± 7
A8	4.3 ± 0.5	A19	31 ± 5
A9	39 ± 2		

[a]Binding affinities of negative controls for this assay were determined in a previous study.[27] [b]The error shown is the standard error based on triplicate experiments.

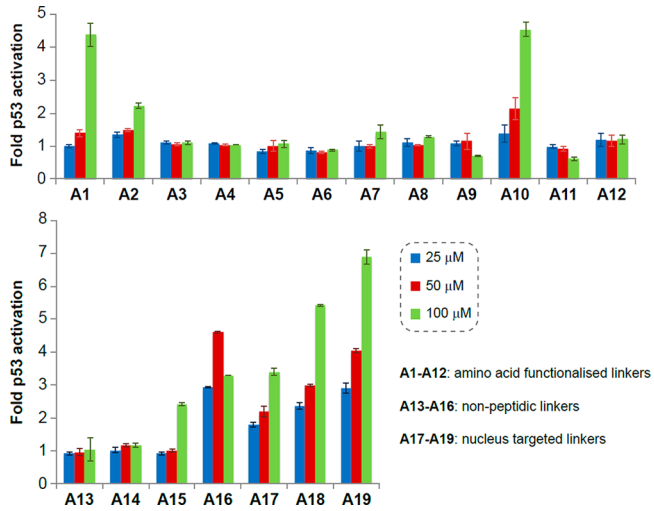

Figure 3. p53 activation for diversified stapled peptides in a T22 mammalian cell reporter assay. Data is reported as fold activation over 1% DMSO vehicle control, with error bars representing the standard deviation of triplicate experiments. The wild-type $p53_{17-29}$ peptide and unstapled peptide **A** are negative controls that both show no activity in this assay.[27]

a potentially important function beyond simply introducing positive charge (Table 1 and Figure 3).

As we postulated that the clear disparity between *in vitro* binding and reporter assay activity was due to changes in peptide uptake, we stapled the N-terminal TAMRA-labeled analogue **B** with linkers **1**, **2**, **3**, **5**, **8**, and **10** (R3/K3/E3/S3/K3-OH/K4, respectively) for qualitative assessment of cell permeability in T22 mammalian cells by fluorescence confocal microscopy. Initially, we had chosen to conduct confocal microscopy on cells which had been fixed with paraformaldehyde prior to imaging, as had been reported in many previous studies on stapled peptide uptake.[9,11,27,39−42] These experiments revealed that only peptides **B1**, **B2**, and **B10** (R3/K3/K4 functionality) had appreciable levels of intracellular fluorescence, directly matching the observations from the p53 reporter assay (Supporting Information Figure S6.1.1).

While the fixed cell experiments appeared to show diffuse peptide localization throughout the cell, we also conducted imaging of live unfixed cells, as fixation has previously been shown to give misleading results in the field of cell-penetrating peptides.[43] Upon direct comparison of images from fixed and nonfixed cells, **B1**, **B2**, and **B10** were still the only peptides that showed appreciable fluorescence. However, the cellular distribution of this fluorescence was markedly different (Figure 4 and Supporting Information Figure S6.2.1). There was a high degree of punctuate fluorescence, which is indicative of peptides being trapped in endosomes or lysosomes following cell entry via an endocytosis-dependent mechanism (with mitochondrial localization a possibility for **B10**). Also notable

DOI: 10.1021/acschembio.9b00063
ACS Chem. Biol. 2019, 14, 526−533

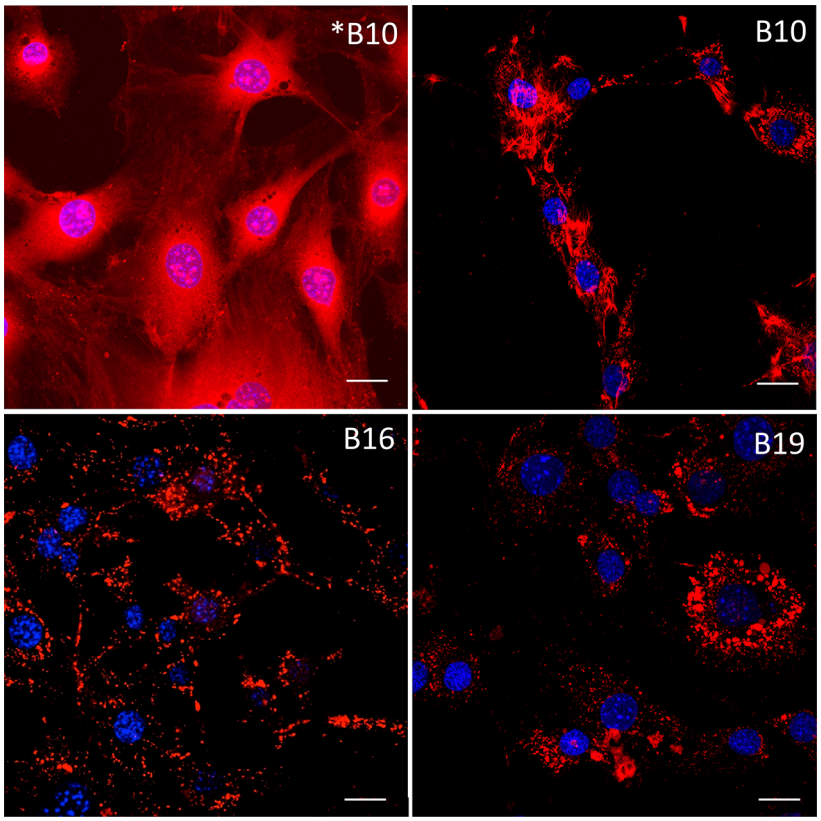

Figure 4. Examples of fixed cell (*B10) and live cell (B10, B16, and B19) confocal fluorescence microscopy images in T22 mammalian cells, with only the live cell images showing punctuated fluorescence indicative of endosomal or lysosomal entrapment. Peptides are shown in red, and Hoechst-stained nuclei are shown in blue. Scale bar: 25 μm. A full set of fixed and live cell images is presented in the Supporting Information (Figures S6.1.1 and S6.2.1).

was the distinct lack of detectable fluorescence in the nucleus, which is critical for inhibition of the nuclear p53/MDM2 interaction.[44,45] These results suggest that although these peptides are taken up sufficiently to elicit a response in a p53 reporter assay, further modifications to promote cytosolic and nuclear delivery of peptides could enhance target engagement and therefore the therapeutic potential of these stapled peptides.

Nonpeptidic Linkers. We designed a second series of linkers **13**−**15** bearing nonpeptidic polyamines to mimic the cell-permeabilizing role of lysine (Figure 2). Despite retaining their *in vitro* binding affinity for MDM2, the polyamine stapled peptides **13A**−**15A** also resulted in loss of activity in cells (Table 1, Figure 3). As the polyamine motifs were protonated under the cellular assay pH, this result confirms that positive charge alone is not a sufficient condition for peptide uptake.

Inspired by the series of small molecule carriers (SMoCs) developed by Selwood and coworkers,[46−48] we also incorporated a SMoC group into the dialkynyl linker **16** (Figure 2). The resulting stapled peptide **A16** gave an enhanced p53 response in comparison to **A1** and **A10** at lower concentrations (25, 50 μM), although a drop in activity was noted at the highest concentration of 100 μM (Figure 3), potentially due to toxicity effects at high concentration. Confocal imaging of the TAMRA labeled analogue **B16** revealed significant punctuation in the fluorescence (Figure 4).

Nucleus-Targeted Linkers. With the aim of promoting peptide delivery into the nucleus, we explored linkers **17**−**19** functionalized with a nuclear localization signal (NLS) sequence PKKKRKV derived from the SV40 Large T-antigen.[49] This sequence is known to bind to the major site on importin α, which facilitates the transport of NLS-containing proteins into the nucleus.[50] A variable number of 6-aminohexanoic acid (Ahx) spacers was inserted to minimize steric clash between the NLS and the MDM2-binding sequence. Stapled peptides **A17**−**A19** showed comparable binding values for MDM2 (Table 1), and the TAMRA labeled versions **B17**−**B19** were found to have submicromolar affinity for importin α in a direct FP assay (**B17**: 81 ± 10 nM, **B18**: 89 ± 7 nM, **B19**: 86 ± 12 nM; Supporting Information Figure S5.2.1).[51] The reporter assay showed greater p53 activation as the number of Ahx spacers increased from one to three, with peptides **A18** and **A19** both showing higher activity compared to **A1** (Figure 3).

Endosomal escape still appears to be a major limiting factor to appropriate target engagement. Confocal imaging of the TAMRA labeled peptide **B19** in T22 mammalian cells indicated a high degree of punctuation was again present in the signal, with minimal fluorescence detected in the nucleus (Figure 4). The subcellular localization of TAMRA labeled peptide **B19** was interrogated in HeLa cells against Lysotracker and Mitotracker labeling. With a Pearson's colocalization coefficient (PCC) of 0.66 (± 0.03) with lysotracker, **B19** exhibited partial lysosomal localization and no significant mitochondrial localization (PCC = 0.01 ± 0.01). This effect appears to be independent of the fluorescent tag or cell line, as similar observations were noted when localization experiments were conducted using the FITC labeled analogue **C19** in HeLa cells. Further fluorescence colocalization imaging with Lysotracker and Mitotracker dyes showed peptide **C19** was

DOI: 10.1021/acschembio.9b00063
ACS Chem. Biol. 2019, 14, 526−533

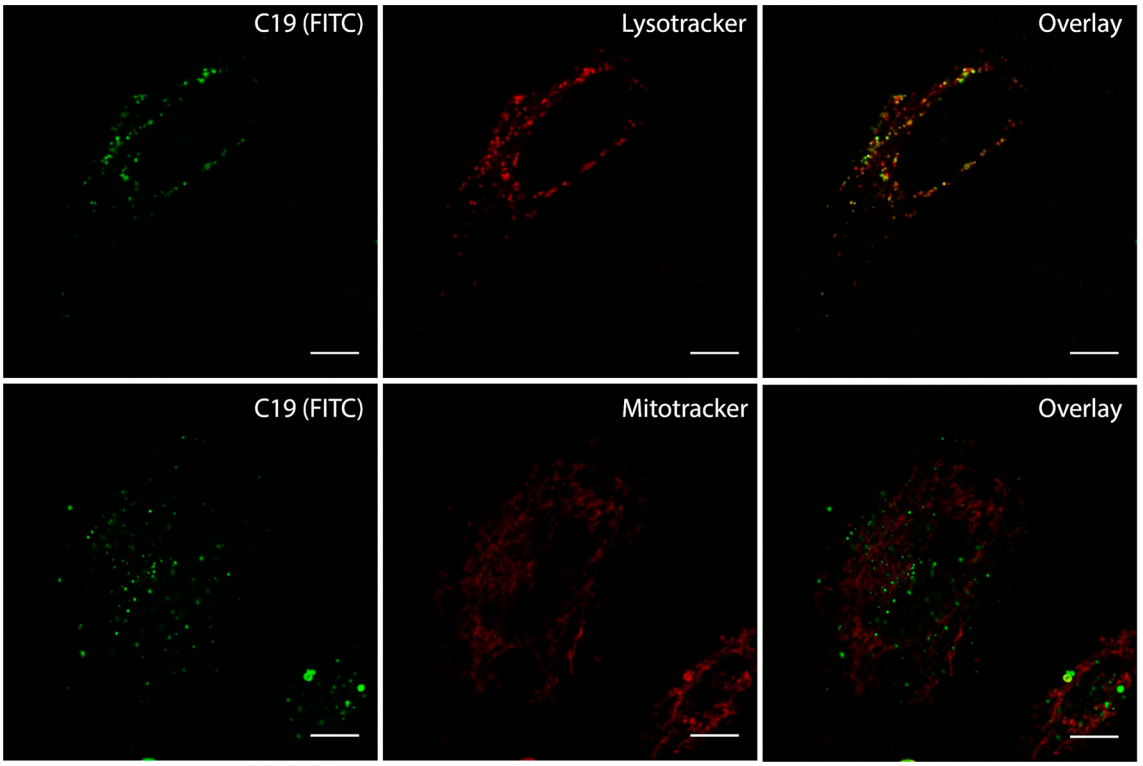

Figure 5. Examples of live cell confocal fluorescence microscopy images in HeLa cells. The top row shows peptide **C19** in green and lysosomes (Lysotracker DeepRed) in red, with significant observable colocalization. The bottom row shows peptide C19 in green and mitochondria (Mitotracker DeepRed) in red, with no significant colocalization. A vehicle-only negative control (DMSO) showed no observable FITC fluorescence. Scale bar: 10 μm. Images for peptide **B19** are shown in the Supporting Information Figure 6.5.1.

partially localized in the lysosomes (PCC = 0.47 ± 0.04) after 1 h incubation with live HeLa cells (Figure 5), with no significant mitochondrial localization (PCC = 0.01 ± 0.01). The results suggest that while the NLS sequence is capable of promoting cellular uptake, presumably by virtue of the positively charged arginine and lysine residues in the sequence, the majority of the administered stapled peptide remains trapped in lysosomal trafficking pathways.

Peptide Sequence Variants. To evaluate if the most promising staple linkers SMoC **16** and NLS-3 **19** (Figure 6) were compatible with different MDM2-binding sequences, we investigated three MDM2-binding sequence variants **D**–**F**. Peptide **D** was derived from the wild type p53-derived sequence without the K24R mutation found in peptide **A**,[52,53] while **E** and **F** were based on the phage-derived PDI peptides previously studied for hydrocarbon stapling.[9] All six compounds retained their binding affinity for MDM2 (Supporting Information Table S3.2.1) and elicited a positive response in the cellular reporter assay (Figure 6). In particular, stapled peptide **F16** induced the greatest activation at the top concentration for the SMoC linker **16** series, while peptide **D19** was superior within the NLS-3 linker **19** series.

We conducted a lactate dehydrogenase (LDH) leakage assay to investigate the possibility that the stapled peptides could cause general cytotoxicity.[54,55] The results were varied, but gratifyingly did not display any clear correlation with observed activity in the p53 reporter assay (Supporting Information Figure 7.1.1). This suggests that unwanted toxicity, independent of any p53-driven mechanism, was occurring with only some of the stapled peptides. In the NLS-3 linker **19** series for example, peptide **A19** exhibited no general toxicity, whereas

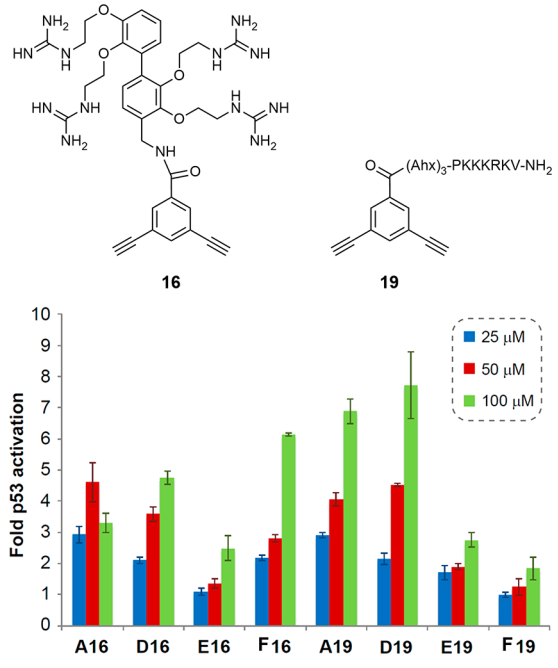

Figure 6. Cellular activity of stapled peptides based on different sequences (**A** and **D**–**F**) combined with linkers **16** and **19** in the cellular p53 reporter assay. Data is reported as fold activation over 1% DMSO control, with error bars representing the standard deviation of triplicate experiments.

9% LDH leakage was detected for **D19** at 100 μM, despite both peptides having comparable activity in the reporter assay. For the SMoC linker **16** series, **F16** showed high levels of

DOI: 10.1021/acschembio.9b00063
ACS Chem. Biol. 2019, 14, 526–533

toxicity at 54% leakage, while the similarly potent peptide **D16** displayed no such toxicity effects. Overall, the NLS-3 stapled peptides with linker **19** were less toxic than the SMoC series with linker **16**. Our findings suggest that nonspecific toxicity arises from a combination of staple linker and peptide sequence and not necessarily either of them in isolation. This feature enabled us to identify suitable combinations **D16** and **A19** that displayed potent cellular activity while eliminating any unwanted toxicity. These peptides were found to have submicromolar affinity for MDMX in a competitive FP assay (**D16**: 71 ± 6 nM, **A19**: 170 ± 10 nM; Supporting Information Figure S4.3.1). Despite the large NLS staple, **A19** also displayed a moderate level of alpha helicity by circular dichroism (Supporting Information Figure S8.2.1).

CONCLUSIONS

We presented a systematic analysis of staple functionality on biological activity using the p53/MDM2 interaction as a model system. Out of the 18 staples, five (**10**, **16**, **17**, **18**, and **19**) were found to be comparable or superior to the first generation activity-enhancing staple **1**. While most of the stapled peptides have similar *in vitro* binding affinities for MDM2, remarkable variability in cellular activity can be attributed to differences in cellular uptake. The two most effective uptake-promoting linkers in this study are SMoC **16** and NLS-3 **19**, although crucially, their activity and toxicity is highly dependent on the match-up with a specific peptide sequence variant. Finally, confocal microscopy experiments indicate that promoting endosomal release and nuclear uptake would further improve the therapeutic potential of these p53-derived stapled peptides.

Lessons from applying this toolbox to a variety of PPIs will help to map out the landscape of physicochemical factors that affect cellular efficacy. This study provides strong evidence that there exists a complex interplay between many physicochemical parameters that determines cellular efficacy, and that subtle changes in either linker or peptide sequence can have a substantial impact on activity. The linker toolbox serves to further our understanding of these influential parameters, toward the ultimate goal of being able to employ more rational optimization strategies when conducting future studies on stapled peptides in the cellular context and beyond.

METHODS

Full experimental methods and characterization data are provided in the Supporting Information.

Fixed Cell Imaging. T22 cells were seeded in an 8-chamber glass slide (8000 cells/chamber in 250 μL, Lab-Tek). Cells were incubated at 37 °C in a 5% CO_2 atmosphere for 24 h before the medium was removed, and new medium containing the fluorescent peptides (20 μM) was added. The cells were incubated for a further 18 h before the medium was removed and cells were washed with 100 μL PBS. The cells were fixed in 100 μL of 4% paraformaldehyde in PBS for 10 min, before being washed twice with 100 μL of PBS. The chambers were then removed and a coverslip with Vectashield mounting medium containing DAPI (Vector Laboratories) was applied. The cells were then imaged on a Leica SP5 confocal microscope using a 63× objective. Final images are generated as a maximum intensity projection of at least ten Z-stacked images.

Live Cell Imaging. T22 cells were seeded in glass-bottom dishes (64 000 cells/dish in 2 mL, Mat-Tek). Cells were incubated at 37 °C in a 5% CO_2 atmosphere for 24 h before the medium was removed, and new medium containing the fluorescent peptides (20 μM in 1 mL) was added. The cells were incubated for a further 3.5 h before Hoechst 33342 dye (4 μg per well) was added to the medium for a further 0.5 h. Cells were then washed with 1 mL PBS before adding fresh Dulbecco's modified Eagle's medium with serum (1 mL) for **B1**−**B10** or Hanks' Balanced Salt Solution without serum (1 mL) for **B15**−**B19**. The cells were then immediately imaged on a Leica SP5 confocal microscope using a 63× objective. Final images are generated as a maximum intensity projection of ten Z-stacked images.

Live Cell Colocalization Imaging. HeLa cells were seeded in glass-bottom dishes (60 000 cells/dish in 2 mL, Mat-Tek). Cells were incubated at 37 °C in a 5% CO_2 atmosphere for 24 h before the medium was removed, and new medium containing the fluorescent peptides (10 μM in 1 mL) was added. The cells were incubated for a further 1 h before Mitotracker DeepRed (250 nM) or Lysotracker DeepRed (250 nM) was added to the medium for a further 5 min. Cells were then washed thrice with 1 mL PBS before adding fresh Dulbecco's modified Eagle's medium (without phenol red). The cells were then immediately imaged on a Leica SP5 confocal microscope equipped with white light laser using a 100× oil objective with a 2× zoom. Images were analyzed using FIJI ImageJ by drawing a region of interest over the entire cell. Colocalization analyses on five independent images were performed using FIJI ImageJ Coloc2 Plugin, and PCC was used to quantify the extent of overlap between the localization of the peptide and the tracker dyes.

ASSOCIATED CONTENT

Supporting Information

The Supporting Information is available free of charge on the ACS Publications website at DOI: 10.1021/acschembio.9b00063.

Synthetic procedures, cellular p53 reporter assay, MDM2 competitive fluorescence polarization, MDMX fluorescence polarization, importin α direct fluorescence polarization, confocal fluorescence microscopy, LDH leakage toxicity assay, circular dichroism, and solubility (PDF)

AUTHOR INFORMATION

Corresponding Authors

*E-mail: yuheng.lau@sydney.edu.au.
*E-mail: spring@ch.cam.ac.uk.

ORCID

Yuteng Wu: 0000-0002-8573-9626
Amandeep Kaur: 0000-0002-0898-875X
Elaine Fowler: 0000-0002-6942-646X
Stephen J. Walsh: 0000-0002-3164-1519
Laura S. Itzhaki: 0000-0001-6504-2576
David R. Spring: 0000-0001-7355-2824

Author Contributions

The research was conceived by Y.H.L. and D.R.S. Synthesis was carried out by Y.W., Y.H.L., E.F., L.O., and P.D.A. Importin assays were conducted by M.M.W. MDMX assays were performed by Y.H.L. and R.Y. p53 assays were conducted by Y.W., Y.H.L., A.C., W.X., and M.J., with support from L.S.I. Microscopy was conducted by A.K., Y.H.L., and Y.W. The manuscript was written by Y.W., Y.H.L., E.F., W.R.J.D.G., H.F.S., T.T.L.K., S.W., and D.R.S.

Notes

The authors declare no competing financial interest.

ACKNOWLEDGMENTS

The Spring laboratory research was supported by grants from the ERC, EPSRC, BBSRC, MRC, and Royal Society. Y.H.L. acknowledges the Cambridge Trusts for funding. M.M.W. acknowledges funding from Cancer Research UK, Department

DOI: 10.1021/acschembio.9b00063
ACS Chem. Biol. 2019, 14, 526−533

of Chemistry at the University of Cambridge, School of the Physical Sciences and the Cambridge Cancer Centre. S.J.W. acknowledges the Cambridge Trusts and AstraZeneca for funding. P.D.A. acknowledges the Conselho Nacional de Desenvolvimento Científico e Tecnológico for funding. L.S.I. was supported by a Senior Fellowship from the Medical Research Foundation, and W.X. by the MRC (G1002329).

REFERENCES

(1) Ryan, D. P., and Matthews, J. M. (2005) Protein−protein interactions in human disease. *Curr. Opin. Struct. Biol. 15*, 441−446.
(2) Ivanov, A. A., Khuri, F. R., and Fu, H. (2013) Targeting protein−protein interactions as an anticancer strategy. *Trends Pharmacol. Sci. 34*, 393−400.
(3) Wells, J. A., and McClendon, C. L. (2007) Reaching for high-hanging fruit in drug discovery at protein−protein interfaces. *Nature 450*, 1001−1009.
(4) Pelay-Gimeno, M., Glas, A., Koch, O., and Grossmann, T. N. (2015) Structure-Based Design of Inhibitors of Protein−Protein Interactions: Mimicking Peptide Binding Epitopes. *Angew. Chem., Int. Ed. 54*, 8896−8927.
(5) Azzarito, V., Long, K., Murphy, N. S., and Wilson, A. J. (2013) Inhibition of α-helix-mediated protein−protein interactions using designed molecules. *Nat. Chem. 5*, 161−173.
(6) Valeur, E., Guéret, S. M., Adihou, H., Gopalakrishnan, R., Lemurell, M., Waldmann, H., Grossmann, T. N., and Plowright, A. T. (2017) New modalities for challenging targets in drug discovery. *Angew. Chem., Int. Ed. 56*, 10294−10323.
(7) Walensky, L. D., and Bird, G. H. (2014) Hydrocarbon-stapled peptides: principles, practice, and progress: miniperspective. *J. Med. Chem. 57*, 6275−6288.
(8) Lau, Y. H., de Andrade, P., Wu, Y., and Spring, D. R. (2015) Peptide stapling techniques based on different macrocyclisation chemistries. *Chem. Soc. Rev. 44*, 91−102.
(9) Chang, Y. S., Graves, B., Guerlavais, V., Tovar, C., Packman, K., To, K.-H., Olson, K. A., Kesavan, K., Gangurde, P., Mukherjee, A., Baker, T., Darlak, K., Elkin, C., Filipovic, Z., Qureshi, F. Z., Cai, H., Berry, P., Feyfant, E., Shi, X. E., Horstick, J., Annis, D. A., Manning, A. M., Fotouhi, N., Nash, H., Vassilev, L. T., and Sawyer, T. K. (2013) Stapled α− helical peptide drug development: A potent dual inhibitor of MDM2 and MDMX for p53-dependent cancer therapy. *Proc. Natl. Acad. Sci. U. S. A. 110*, E3445−E3454.
(10) Moellering, R. E., Cornejo, M., Davis, T. N., Del Bianco, C., Aster, J. C., Blacklow, S. C., Kung, A. L., Gilliland, D. G., Verdine, G. L., and Bradner, J. E. (2009) Direct inhibition of the NOTCH transcription factor complex. *Nature 462*, 182−188.
(11) Walensky, L. D., Kung, A. L., Escher, I., Malia, T. J., Barbuto, S., Wright, R. D., Wagner, G., Verdine, G. L., and Korsmeyer, S. J. (2004) Activation of apoptosis in vivo by a hydrocarbon-stapled BH3 helix. *Science 305*, 1466−1470.
(12) Rennie, Y. K., McIntyre, P. J., Akindele, T., Bayliss, R., and Jamieson, A. G. (2016) A TPX2 proteomimetic has enhanced affinity for Aurora-A due to hydrocarbon stapling of a helix. *ACS Chem. Biol. 11*, 3383−3390.
(13) Bird, G. H., Mazzola, E., Opoku-Nsiah, K., Lammert, M. A., Godes, M., Neuberg, D. S., and Walensky, L. D. (2016) Biophysical determinants for cellular uptake of hydrocarbon-stapled peptide helices. *Nat. Chem. Biol. 12*, 845−852.
(14) Bird, G. H., Crannell, W. C., and Walensky, L. D. (2011) Chemical Synthesis of Hydrocarbon-Stapled Peptides for Protein Interaction Research and Therapeutic Targeting. *Curr. Protoc. Chem. Biol. 3*, 99−117.
(15) Chu, Q., Moellering, R. E., Hilinski, G. J., Kim, Y.-W., Grossmann, T. N., Yeh, J. T.-H., and Verdine, G. L. (2015) Towards understanding cell penetration by stapled peptides. *MedChemComm 6*, 111−119.
(16) Sun, T.-L., Sun, Y., Lee, C.-C., and Huang, H. W. (2013) Membrane permeability of hydrocarbon-cross-linked peptides. *Biophys. J. 104*, 1923−1932.
(17) Welser, K., Campbell, F., Kudsiova, L., Mohammadi, A., Dawson, N., Hart, S. L., Barlow, D. J., Hailes, H. C., Lawrence, M. J., and Tabor, A. B. (2013) Gene delivery using ternary lipopolyplexes incorporating branched cationic peptides: the role of peptide sequence and branching. *Mol. Pharmaceutics 10*, 127−141.
(18) Peraro, L., and Kritzer, J. A. (2018) Emerging Methods and Design Principles for Cell-Penetrant Peptides. *Angew. Chem., Int. Ed. 57*, 11868−11881.
(19) Brown, S. P., and Smith, A. B. (2015) Peptide/Protein Stapling and Unstapling: Introduction of s-Tetrazine, Photochemical Release, and Regeneration of the Peptide/Protein. *J. Am. Chem. Soc. 137*, 4034−4037.
(20) Nevola, L., Martín-Quirós, A., Eckelt, K., Camarero, N., Tosi, S., Llobet, A., Giralt, E., and Gorostiza, P. (2013) Light-Regulated Stapled Peptides to Inhibit Protein−Protein Interactions Involved in Clathrin-Mediated Endocytosis. *Angew. Chem., Int. Ed. 52*, 7704−7708.
(21) Grison, C. M., Burslem, G. M., Miles, J. A., Pilsl, L. K. A., Yeo, D. J., Imani, Z., Warriner, S. L., Webb, M. E., and Wilson, A. J. (2017) Double quick, double click reversible peptide "stapling. *Chem. Sci. 8*, 5166−5171.
(22) Peraro, L., Zou, Z., Makwana, K. M., Cummings, A. E., Ball, H. L., Yu, H., Lin, Y.-S., Levine, B., and Kritzer, J. A. (2017) Diversity-Oriented Stapling Yields Intrinsically Cell-Penetrant Inducers of Autophagy. *J. Am. Chem. Soc. 139*, 7792−7802.
(23) Xu, W., Lau, Y. H., Fischer, G., Tan, Y. S., Chattopadhyay, A., de la Roche, M., Hyvönen, M., Verma, C., Spring, D. R., and Itzhaki, L. S. (2017) Macrocyclized extended peptides: inhibiting the substrate-recognition domain of tankyrase. *J. Am. Chem. Soc. 139*, 2245−2256.
(24) Tian, Y., Jiang, Y., Li, J., Wang, D., Zhao, H., and Li, Z. (2017) Effect of Stapling Architecture on Physiochemical Properties and Cell Permeability of Stapled α-Helical Peptides: A Comparative Study. *ChemBioChem 18*, 2087−2093.
(25) Schafmeister, C. E., Po, J., and Verdine, G. L. (2000) An all-hydrocarbon cross-linking system for enhancing the helicity and metabolic stability of peptides. *J. Am. Chem. Soc. 122*, 5891−5892.
(26) Blackwell, H. E., and Grubbs, R. H. (1998) Highly efficient synthesis of covalently cross-linked peptide helices by ring-closing metathesis. *Angew. Chem., Int. Ed. 37*, 3281−3284.
(27) Lau, Y. H., de Andrade, P., Quah, S.-T., Rossmann, M., Laraia, L., Sköld, N., Sum, T. J., Rowling, P. J. E., Joseph, T. L., Verma, C., Hyvönen, M., Itzhaki, L. S., Venkitaraman, A. R., Brown, C. J., Lane, D. P., and Spring, D. R. (2014) Functionalised staple linkages for modulating the cellular activity of stapled peptides. *Chem. Sci. 5*, 1804−1809.
(28) Tran, P. T., Larsen, C. Ø., Røndbjerg, T., De Foresta, M., Kunze, M. B. A., Marek, A., Løper, J. H., Boyhus, L.-E., Knuhtsen, A., Lindorff-Larsen, K., and Pedersen, D. S. (2017) Diversity-Oriented Peptide Stapling: A Third Generation Copper-Catalysed Azide−Alkyne Cycloaddition Stapling and Functionalisation Strategy. *Chem. - Eur. J. 23*, 3490−3495.
(29) Serrano, J. C., Sipthorp, J., Xu, W., Itzhaki, L. S., and Ley, S. V. (2017) A new methodology for incorporating chiral linkers into stapled peptides. *ChemBioChem 18*, 1066−1071.
(30) Wang, Y., and Chou, D. H.-C. (2015) A thiol−ene coupling approach to native peptide stapling and macrocyclization. *Angew. Chem., Int. Ed. 54*, 10931−10934.
(31) Gimenez, D., Mooney, C. A., Dose, A., Sandford, G., Coxon, C. R., and Cobb, S. L. (2017) The application of perfluoroheteroaromatic reagents in the preparation of modified peptide systems. *Org. Biomol. Chem. 15*, 4086−4095.
(32) Lau, Y. H., Wu, Y., de Andrade, P., Galloway, W. R. J. D., and Spring, D. R. (2015) A two-component'double-click'approach to peptide stapling. *Nat. Protoc. 10*, 585−594.

DOI: 10.1021/acschembio.9b00063
ACS Chem. Biol. 2019, 14, 526−533

(33) Brown, C. J., Lain, S., Verma, C. S., Fersht, A. R., and Lane, D. P. (2009) Awakening guardian angels: drugging the p53 pathway. *Nat. Rev. Cancer 9*, 862−873.
(34) Kussie, P. H., Gorina, S., Marechal, V., Elenbaas, B., Moreau, J., Levine, A. J., and Pavletich, N. P. (1996) Structure of the MDM2 oncoprotein bound to the p53 tumor suppressor transactivation domain. *Science 274*, 948−953.
(35) Lau, Y. H., de Andrade, P., McKenzie, G. J., Venkitaraman, A. R., and Spring, D. R. (2014) Linear Aliphatic Dialkynes as Alternative Linkers for Double-Click Stapling of p53-Derived Peptides. *ChemBioChem 15*, 2680−2683.
(36) Iegre, J., Ahmed, N. S., Gaynord, J. S., Wu, Y., Herlihy, K. M., Tan, Y. S., Lopes-Pires, M. E., Jha, R., Lau, Y. H., Sore, H., Verma, C., O'Donovan, D. H., Pugh, N., and Spring, D. R. (2018) Stapled peptides as a new technology to investigate protein−protein interactions in human platelets. *Chem. Sci. 9*, 4638−4643.
(37) Brown, C. J., Quah, S. T., Jong, J., Goh, A. M., Chiam, P. C., Khoo, K. H., Choong, M. L., Lee, M. A., Yurlova, L., Zolghadr, K., Joseph, T. L., Verma, C. S., and Lane, D. P. (2013) Stapled peptides with improved potency and specificity that activate p53. *ACS Chem. Biol. 8*, 506−512.
(38) Muppidi, A., Doi, K., Edwardraja, S., Drake, E. J., Gulick, A. M., Wang, H.-G., and Lin, Q. (2012) Rational design of proteolytically stable, cell-permeable peptide-based selective Mcl-1 inhibitors. *J. Am. Chem. Soc. 134*, 14734−14737.
(39) Frank, A. O., Vangamudi, B., Feldkamp, M. D., Souza-Fagundes, E. M., Luzwick, J. W., Cortez, D., Olejniczak, E. T., Waterson, A. G., Rossanese, O. W., Chazin, W. J., and Fesik, S. W. (2014) Discovery of a potent stapled helix peptide that binds to the 70N domain of replication protein A. *J. Med. Chem. 57*, 2455−2461.
(40) Tan, B. X., Brown, C. J., Ferrer, F. J., Yuen, T. Y., Quah, S. T., Chan, B. H., Jansson, A. E., Teo, H. L., Nordlund, P., and Lane, D. P. (2015) Assessing the efficacy of Mdm2/Mdm4-inhibiting stapled peptides using cellular thermal shift assays. *Sci. Rep. 5*, 12116.
(41) Cromm, P. M., Spiegel, J., Küchler, P., Dietrich, L., Kriegesmann, J., Wendt, M., Goody, R. S., Waldmann, H., and Grossmann, T. N. (2016) Protease-resistant and cell-permeable double-stapled peptides targeting the Rab8a GTPase. *ACS Chem. Biol. 11*, 2375−2382.
(42) Thomas, J. C., Cooper, J. M., Clayton, N. S., Wang, C., White, M. A., Abell, C., Owen, D., and Mott, H. R. (2016) Inhibition of Ral GTPases using a stapled peptide approach. *J. Biol. Chem. 291*, 18310−18325.
(43) Richard, J. P., Melikov, K., Vives, E., Ramos, C., Verbeure, B., Gait, M. J., Chernomordik, L. V., and Lebleu, B. (2003) Cell-penetrating peptides A reevaluation of the mechanism of cellular uptake. *J. Biol. Chem. 278*, 585−590.
(44) Uhlen, M., Oksvold, P., Fagerberg, L., Lundberg, E., Jonasson, K., Forsberg, M., Zwahlen, M., Kampf, C., Wester, K., Hober, S., Wernerus, H., Bjorling, L., and Ponten, F. (2010) Towards a knowledge-based human protein atlas. *Nat. Biotechnol. 28*, 1248−1250.
(45) Uhlén, M., Björling, E., Agaton, C., Szigyarto, C. A.-K., Amini, B., Andersen, E., Andersson, A.-C., Angelidou, P., Asplund, A., Asplund, C., Berglund, L., Bergström, K., Brumer, H., Cerjan, D., Ekström, M., Elobeid, A., Eriksson, C., Fagerberg, L., Falk, R., Fall, J., Forsberg, M., Björklund, M. G., Gumbel, K., Halimi, A., Hallin, I., Hamsten, C., Hansson, M., Hedhammar, M., Hercules, G., Kampf, C., Larsson, K., Lindskog, M., Lodewyckx, W., Lund, J., Lundeberg, J., Magnusson, K., Malm, E., Nilsson, P., Ödling, J., Oksvold, P., Olsson, I., Öster, E., Ottosson, J., Paavilainen, L., Persson, A., Rimini, R., Rockberg, J., Runeson, M., Sivertsson, Å., Sköllermo, A., Steen, J., Stenvall, M., Sterky, F., Strömberg, S., Sundberg, M., Tegel, H., Tourle, S., Wahlund, E., Waldén, A., Wan, J., Wernérus, H., Westberg, J., Wester, K., Wrethagen, U., Xu, L. L., Hober, S., and Pontén, F. (2005) A human protein atlas for normal and cancer tissues based on antibody proteomics. *Mol. Cell. Proteomics 4*, 1920−1932.
(46) Gooding, M., Adigbli, D., Edith Chan, A. W., Melander, R. J., MacRobert, A. J., and Selwood, D. L. (2014) A Bifurcated Proteoglycan Binding Small Molecule Carrier for si RNA Delivery. *Chem. Biol. Drug Des. 84*, 24−35.
(47) Rebstock, A., Visintin, C., Leo, E., Garcia Posada, C., Kingsbury, S. R., Williams, G. H., Stoeber, K., and Selwood, D. L. (2008) Modular assembly using sequential palladium coupling gives easy access to the SMoC class of cellular transporters. *ChemBioChem 9*, 1787−1796.
(48) Okuyama, M., Laman, H., Kingsbury, S. R., Visintin, C., Leo, E., Eward, K. L., Stoeber, K., Boshoff, C., Williams, G. H., and Selwood, D. L. (2007) Small-molecule mimics of an α-helix for efficient transport of proteins into cells. *Nat. Methods 4*, 153−159.
(49) Kalderon, D., Roberts, B. L., Richardson, W. D., and Smith, A. E. (1984) A short amino acid sequence able to specify nuclear location. *Cell 39*, 499−509.
(50) Conti, E., and Kuriyan, J. (2000) Crystallographic analysis of the specific yet versatile recognition of distinct nuclear localization signals by karyopherin α. *Structure 8*, 329−338.
(51) Wiedmann, M. M., Tan, Y. S., Wu, Y., Aibara, S., Xu, W., Sore, H. F., Verma, C. S., Itzhaki, L., Stewart, M., Brenton, J. D., and Spring, D. R. (2017) Development of Cell-Permeable, Non-Helical Constrained Peptides to Target a Key Protein−Protein Interaction in Ovarian Cancer. *Angew. Chem., Int. Ed. 56*, 524−529.
(52) Bernal, F., Tyler, A. F., Korsmeyer, S. J., Walensky, L. D., and Verdine, G. L. (2007) Reactivation of the p53 tumor suppressor pathway by a stapled p53 peptide. *J. Am. Chem. Soc. 129*, 2456−2457.
(53) Lau, Y. H., de Andrade, P., Skold, N., McKenzie, G. J., Venkitaraman, A. R., Verma, C., Lane, D. P., and Spring, D. R. (2014) Investigating peptide sequence variations for 'double-click'stapled p53 peptides. *Org. Biomol. Chem. 12*, 4074−4077.
(54) Li, Y.-C., Rodewald, L. W., Hoppmann, C., Wong, E. T., Lebreton, S., Safar, P., Patek, M., Wang, L., Wertman, K. F., and Wahl, G. M. (2014) A versatile platform to analyze low-affinity and transient protein-protein interactions in living cells in real time. *Cell Rep. 9*, 1946−1958.
(55) Jones, S. W., Christison, R., Bundell, K., Voyce, C. J., Brockbank, S. M. V, Newham, P., and Lindsay, M. A. (2005) Characterisation of cell-penetrating peptide-mediated peptide delivery. *Br. J. Pharmacol. 145*, 1093−1102.

DOI: 10.1021/acschembio.9b00063
ACS Chem. Biol. 2019, 14, 526−533